particles

MDPI

Article

The Transmission Muography Technique for Locating Potential Radon Gas Conduits at the Temperino Mine (Tuscany, Italy) †

Diletta Borselli [1,2,*], Tommaso Beni [2,3], Lorenzo Bonechi [2], Debora Brocchini [4], Nicola Casagli [3], Roberto Ciaranfi [2], Vitaliano Ciulli [1,2], Raffaello D'Alessandro [1,2], Andrea Dini [5], Catalin Frosin [1,2], Giovanni Gigli [3], Sandro Gonzi [1,2], Silvia Guideri [4], Luca Lombardi [3], Massimiliano Nocentini [3], Andrea Paccagnella [1,2] and Simone Vezzoni [5]

1 Department of Physics and Astronomy, University of Florence, Via Giovanni Sansone 1, 50019 Sesto Fiorentino, Italy; vitaliano.ciulli@unifi.it (V.C.); raffaello.dalessandro@unifi.it (R.D.); catalin.frosin@unifi.it (C.F.); sandro.gonzi@unifi.it (S.G.); andre.paccagnella@unifi.it (A.P.)
2 National Institute for Nuclear Physics, Division of Florence, Via Bruno Rossi 1, 50019 Sesto Fiorentino, Italy; tommaso.beni@unifi.it (T.B.); lorenzo.bonechi@fi.infn.it (L.B.); roberto.ciaranfi@fi.infn.it (R.C.)
3 Department of Earth Sciences, University of Florence, Via Giorgio La Pira 4, 50121 Florence, Italy; nicola.casagli@unifi.it (N.C.); giovanni.gigli@unifi.it (G.G.); luca.lombardi@unifi.it (L.L.); massimiliano.nocentini@unifi.it (M.N.)
4 Parchi Val di Cornia S.p.A., Via Leonardo da Vinci 13, 57025 Piombino, Italy; brocchini@parchivaldicornia.it (D.B.); guideris@parchivaldicornia.it (S.G.)
5 Institute of Geosciences and Earth Resources, National Research Council of Italy, Via Giuseppe Moruzzi 1, 56124 Pisa, Italy; a.dini@igg.cnr.it (A.D.); simone.vezzoni@igg.cnr.it (S.V.)
* Correspondence: diletta.borselli@fi.infn.it
† This paper is based on the talk at the 13th International Conference on New Frontiers in Physics (ICNFP 2024), Crete, Greece, 26 August–4 September 2024.

Abstract: Transmission muography is an imaging technique that allows us to obtain two-dimensional and three-dimensional average-target density images by measuring the transmission of atmospheric muons. Through this technique, it is possible to observe density anomalies inside a target volume and locate them three-dimensionally. In this work, the potential of the technique will be illustrated through the description of the results of two measurements carried out in the tourist path of the Temperino mine (Livorno, Italy) in an area where a higher concentration of Radon gas is measured. This section of the gallery, located at a depth of about 50 m and dating back to the Etruscan period, might contain ancient cavities not yet discovered that could represent preferential conduits into which Radon gas is released into the tourist route. The muographic results are illustrated, focusing on the search for low-density anomalies attributable to cavities. The measurements are part of the MIMA-SITES project aimed at ensuring the safety of specific zones within the Temperino mine.

Keywords: experimental particle physics; muons; cosmic rays; transmission muography; imaging technique; mine; cavities

check for updates

Academic Editors: Larissa Bravina, Sonia Kabana and Armen Sedrakian

Received: 24 December 2024
Revised: 4 January 2025
Accepted: 8 January 2025
Published: 11 January 2025

Citation: Borselli, D.; Beni, T.; Bonechi, L.; Brocchini, D.; Casagli, N.; Ciaranfi, R.; Ciulli, V.; D'Alessandro, R.; Dini, A.; Frosin, C.; et al. The Transmission Muography Technique for Locating Potential Radon Gas Conduits at the Temperino Mine (Tuscany, Italy). *Particles* **2025**, *8*, 3. https://doi.org/10.3390/particles8010003

1. Introduction

The transmission muography technique [1,2] exploits the penetrating power of atmospheric muons to create images of large targets such as volcanoes, pyramids and archaeological or geological sites [3–10]. Atmospheric muons are generated by the interaction of primary cosmic rays [11] with the nuclei of the atmosphere of the Earth, and are present at the sea level in the vertical direction with a rate of about 70 s^{-1} per square meter [12]. The flux increases with altitude and decreases as a function of the zenith angle θ as $\cos^n(\theta)$ where n depends on the muon energy range (for $E_\mu \simeq 3\,\text{GeV}$, $n = 2$). The muon energy spectrum peaks at about 3 ÷ 4 GeV and extends from hundreds of MeV up to a few TeV. Compared to other particles produced in the atmosphere (i.e., protons, neutrons, electrons, photons, nuclei, neutrinos, kaons and pions) by primary cosmic rays, muons are the most abundantly charged particle at the ground level (for $E_\mu > 1$ GeV) and are also the only one that can penetrate significantly through materials (up to hundreds of meters of rock). The main contribution to energy loss during the interaction with matter is by ionization. Radiative contributions become dominant at momenta above 100 GeV/c [12].

The transmission muography technique exploits the penetrating power of muons by measuring the number of particles transmitted or absorbed by the target to create two-dimensional images of its inner parts, indicating any anomalies. Currently, the technique has spread in many fields: geological and mining for the search for cavities or dense bodies [6,7,13–15], archaeological for the search for tombs or cavities [4,9,10,16], industrial for monitoring blast furnaces or nuclear waste [17–21], and civil security for dams, bridges, and building monitoring.

In this work, transmission muography was applied in the Archaeological and Mining Park of San Silvestro (Campiglia Marittima, Tuscany, Italy) [22,23], which is part of the Parchi Val di Cornia system. The San Silvestro Park preserves abundant traces of historical mining activities, particularly focused on copper, lead and silver extraction. The mining activity ended with the closure of the Temperino mine in 1976 [24]. Among the most distinctive attractions of the park, it is possible to visit the first level of the mine, allowing visitors to immerse themselves in the geological history of the area. In the gallery opened to the public, which reaches a maximum depth of 50 m, annual checks are carried out on the concentration of Radon gas. Radon gas is naturally produced by rocks through the decay chain of uranium. The products of its decay are also radioactive and are fixed in the atmospheric dust, leading to a correlation between exposure to Radon and lung cancer. In closed environments, it is important to keep its concentration under control, because if it exceeds a certain limit, it becomes dangerous for human health. Inside a mine, its presence is natural and can be higher than in cellars or buildings. These checks at the Temperino mine touristic path showed that, in a particular area, there is a higher concentration (always within the safety limits). This area also corresponds to an area of Etruscan ancient excavations where there may be unknown cavities.

The muography technique is employed in this context to search for any undiscovered cavities in the rock layer between the tourist gallery and the Earth's surface. These ancient cavities could represent a source of Radon gas that could enter the tourist route through small conduits (such as fractures). In a muographic image, as will be explained in Section 2.1, the cavities can be seen as angular regions with higher muon counts or, after comparison with simulations, as regions with low density compared to the typical densities of the rocks present in the mine.

2. Materials and Methods

2.1. The Muon Transmission Imaging Technique

Transmission muography allows us, in a non-invasive way, to obtain two-dimensional or three-dimensional images of the target internal structure by measuring the muon transmission. By comparing with simulations, the measured transmission can be converted into an average density value, obtaining an image of the target density. To obtain the measured muon transmission, two muographic measurements need to be performed: one in the presence of the target and one in the absence of the target. The latter serves as a normalization factor for the target flux and to remove the dependence on the detector's geometry and efficiency.

The muon flux $\Phi(\theta, \varphi, S, t)$ detected on a sensitive surface S at the time t in a solid angle $\Delta\Omega$ centered in the direction (θ, φ), with the zenith angle θ and the azimuth angle φ, is defined as:

$$\Phi(\theta, \varphi, S, t) = \frac{N(\theta, \varphi)}{\Delta t A_{eff}(\theta, \varphi, S)\varepsilon(\theta, \varphi)\Delta\Omega} \quad (1)$$

where $N(\theta, \varphi)$ is the number of muons that are detected, $A_{eff} = S \cdot cos(\theta)$ is the detector effective surface in the direction perpendicular to the observation direction and ε is the detector's efficiency. The measured muon transmission T_{meas} can be expressed as a ratio of counts between the two measurements normalized to the acquisition times Δt (once the number of counts has been corrected for the efficiency):

$$T_{meas}(\theta, \varphi) = \frac{N_{target}(\theta, \varphi)}{N_{no-target}(\theta, \varphi)} \frac{\Delta t_{no-target}}{\Delta t_{target}}. \quad (2)$$

Through a simulation that contains the known geometric structure of the target and a cosmic ray flux model on the ground, we obtain the expected muon transmission $T_{exp}(\theta, \varphi, \rho)$, which, in turn, depends on the expected target density ρ, settable via software. By varying the target density in the simulation so as to obtain an expected transmission equal to the measured one, we obtain the average density $\overline{\rho}(\theta, \varphi)$ associated with the target in the direction (θ, φ). Through these steps, we create a two-dimensional angular target's average density distribution. The density observed in each direction is the average density of all the materials that the muon passed through.

To obtain three-dimensional information, several measurements can be taken at different points in the same measurement site and the triangulation or inversion algorithms can be applied [25]. When it is not possible to take more than one measurement, the back-projection algorithm can be used [26] and it allows us to extract three-dimensional information from a single measurement [14]. This algorithm has already been successfully applied to the Temperino mine for the localization of cavities [14] and ore bodies [13].

2.2. The MIMA Muon Tracker

The detectors employed in transmission muography measurements are charged particle trackers. The detector used for this case study is MIMA (Muon Imaging for Mining and Archaeology) [27] assembled at the National Institute for Nuclear Physics (INFN) in Florence. MIMA is a cube of 50 cm per side with a rotating platform, allowing us to define the orientation in elevation and azimuth. The small size allows for easy installation in small and narrow places. MIMA consists of plastic scintillator bars assembled in such a way as to have three tracking planes XY with an angular resolution of 0.3°. Details of the detector can be found in [27]. With the MIMA tracker, it is possible to reconstruct the muon track and count, in each direction that falls inside its acceptance, the number of muons $N(\theta, \varphi)$ that arrive on the detector.

2.3. The Case Study of the Temperino Mine

The mining activity at the Temperino mine (Campiglia Marittima, province of Livorno) [28] dates back to at least the Etruscan period and was then developed intermittently during the Middle Ages [29], the Renaissance and the Industrial Revolution, until its definitive closure in 1976 [24]. The ore bodies were exploited for different commodities such as Cu, Pb, Zn and Ag.

Currently, the Temperino mine has several levels that are located at different depths below the Earth's surface (Figure 1a). The most superficial level (50 m deep) about 360 m long is now used as a tourist route. The mine has been the subject of in-depth geological studies [30] that have allowed for the creation of three-dimensional models of the stratification of the rock overburden. In the area of the Temperino mine, there are calcareous rocks with a density of $2.4 \div 2.7\,\mathrm{g/cm^3}$, porphyries with a density of $2.5 \div 3\,\mathrm{g/cm^3}$, skarn rock with a density of $3.3 \div 3.7\,\mathrm{g/cm^3}$ and other rocks associated with high-density ore minerals such as magnetite, pyrite, chalcopyrite, galena and sphalerite [13].

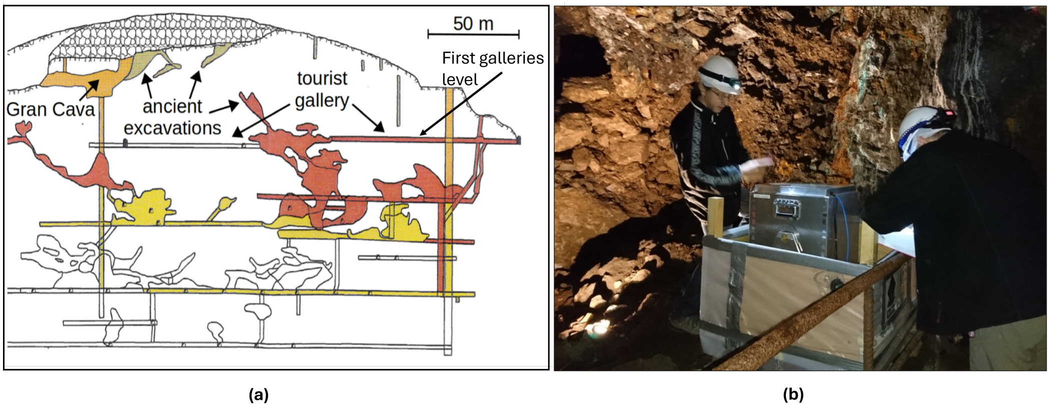

Figure 1. (**a**) The section of the Temperino mine where several levels are visible. At the first level (enclosed by a blue dotted line), there is the tourist path where the muographic measurements were carried out. (**b**) A photograph of the detector installation in the area with the highest concentration of Radon gas.

In the uppermost part of the mine, between the tourist route and the surface, there are ancient Etruscan excavation voids and a large tunnel called Gran Cava, which has two surface entrances. The presence of ancient shafts, excavated in a more or less vertical manner to follow the development of the deposit, was crucial for geologists and mining engineers who resumed mining exploration in the 19th century, further developing it in depth. The intensification of the latest mining activities to provide access to the deepest parts, partially obliterated traces of ancient workings but did not entirely erase them, allowing for the recovery, safeguarding and enhancement of the most significant archaeological and mining features of the area, ultimately leading to the creation of the park. The location of ancient unmapped cavities in this layer would be important not only for archaeological reasons but also for the safety of the tourist route. In fact, any cavities above the tourist route can be included in the calculation of the stress and strain that they cause on the tourist route, indicating the critical points where possible fractures or small landslides may occur.

During the periodic checks of Radon gas emissions within the tourist route of the Temperino mine, it emerged that in a particular area of the mine, there is a greater concentration of this gas (within safety limits). Radon gas has a high permeability and is highly harmful if present in high concentrations. It is therefore good practice to monitor its concentration in every closed environment, in particular in a touristic gallery in which rocks represent sources of this gas. The Temperino gallery is well ventilated, but it could be connected through small cracks to hidden cavities inside which Radon gas might develop in high concentrations. This area of the tourist route is located below an area that we know to have been subject of ancient excavations dating back to the Etruscan era. The presence of cavities located above the tourist route could explain the different concentrations of Radon with respect to the other areas of the mine.

3. Results

3.1. Muographic Measurements at the Temperino Mine

Within the tourist route of the Temperino mine over the years (from 2018 to 2023), seven muographic measurements were carried out. Some of these were focused in an area where the known Gran Cava cavity is visible. These measurements were used to test the technique and test three-dimensional reconstruction algorithms on low- and high-density signals [13,14].

The measurements 4 and 7 were performed in the area of the greatest presence of Radon gas, which is the subject of this article (Figure 1b). The numbering follows the chronological order of the measurements. The area of interest is located approximately halfway along the tourist route near the area called "pillar chamber"where the measurements 4 and 7 were taken (Figure 2a).

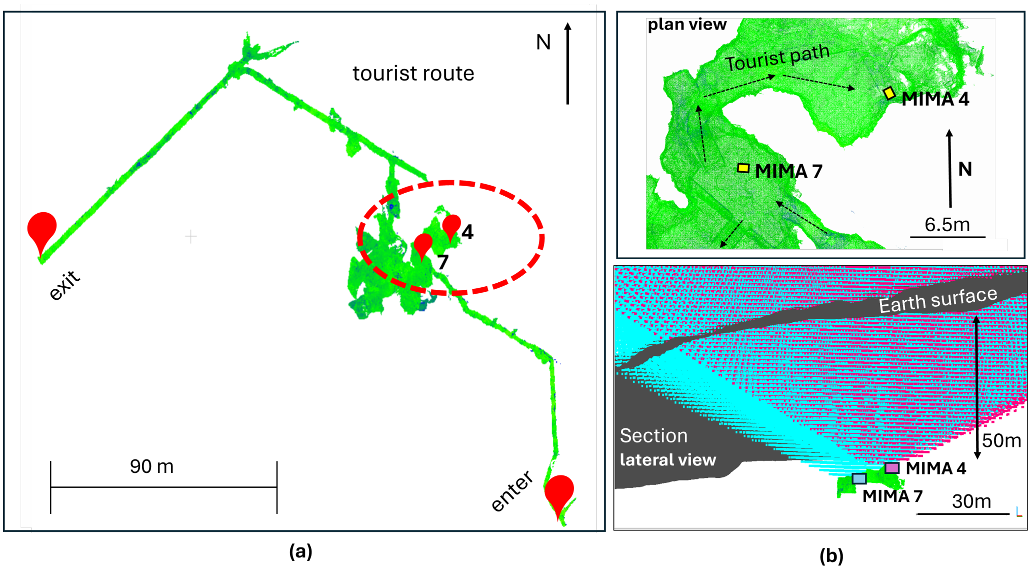

Figure 2. (**a**) The muographic measurement positions within the tourist route for the localization of cavities attributable to the greater presence of Radon gas. The green point cloud was acquired with a laser scanner. (**b**) At the top, the detail of the reciprocal position of the two measurements; at the bottom, the acceptance cones of the detector from the two chosen installation points.

In Figure 2b, at the top, details of the mutual distance of the two detector's positions are shown. The difference in height is about 7 m, with point 4 being higher than point 7. The installation points were chosen so as not to obstruct the tourist path and to be able to observe as much as possible the same angular regions from the two different points of view, as shown in Figure 2b at the bottom, to eventually apply the three-dimensional reconstruction algorithms described in Section 2.1. In both measurements, the detector was pointed vertically.

3.2. Identification of Low-Density Anomalies with the Muon Imaging Technique

The two muographic measurements lasted about 1 month with a rate of approximately 0.5 Hz and were compared with a free-sky measurement carried out on the roof of the INFN building in Florence for a duration of approximately 2 weeks with an acquisition rate of about 19 Hz.

The simulations were carried out using the known geometry of the mine and the geometry of the tourist route. These geometries were acquired by means of unmanned close-range methods in collaboration with the Department of Earth Sciences of the University of Florence. It is very important to include a known detailed geometry in the simulations in order not to have artifacts or false positives in the search for cavities during the comparison with the measurements [8].

By comparing the acquired data with the simulations, following the procedure described in Section 2.1, the two-dimensional angular average-density distributions of Figure 3a,b were obtained from the two measurements.

The two maps are represented in angular coordinates and the center corresponds to the vertical direction. Comparing the density values obtained with the density of the rocks present in the Temperino mine (described in Section 2.3), which are in the range 2.4–5.2 g/cm^3, some areas of lower density can be identified in both maps (surrounded by a white dotted line). These angular regions have been identified as low-density anomalies attributable to hidden cavities that are located above the tourist route.

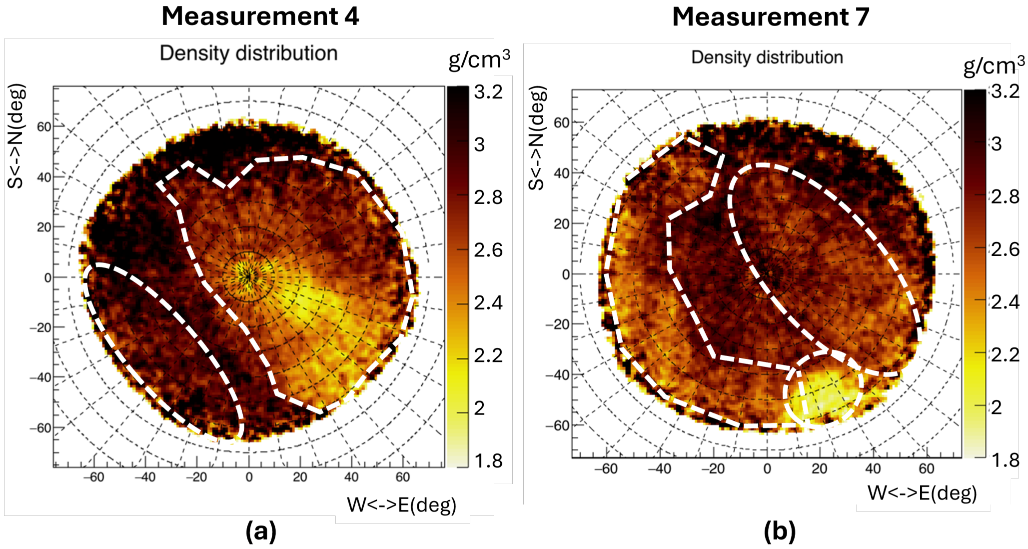

Figure 3. (**a**) and (**b**), respectively, the two-dimensional average-angular-density distributions obtained from the installation points 4 and 7. The observed low-density angular regions attributable to possible cavities are enclosed within white lines.

In the angular distribution obtained from measurement point 4 (Figure 3a), some low-density signals are observed: one inside an area with density of about 2.5 g/cm^3, with the lowest density values (2.2 ÷ 2.3 g/cm^3), that starts from the center (i.e., the detector vertical direction) and extends in the south–east direction; the other one that follows the edge of the detector acceptance between west and south. In the distribution obtained from measurement point 7, three low-density anomalies are identified: one at the edges of the acceptance that extends from west to south; one at low elevations that is located at azimuth angles of 150–170° with the lowest density values (1.9 ÷ 2.0 g/cm^3) and one with the same south–east orientation as the first cavity observed from measurement 4.

The two muographic measurements therefore show the presence of two or more cavities above the Temperino tourist route, which had not yet been identified and which could be linked to the higher levels of Radon gas in this area of the tourist route. The two maps provide only an angular two-dimensional localization of the cavities; to be able to locate them in three dimensions and to understand if the cavities observed by the two measurements are the same, it is necessary to apply the 3D reconstruction algorithms mentioned in Section 2.1.

4. Discussion

This study includes many areas of application: archaeology, mining and civil security. The technique used is the transmission muography that non-invasively—through muon transmission measurements—creates images of the target's inner parts. The case study is the Temperino mine located in Tuscany (Italy). The first level of this mine intersects Etruscan mining excavations, which are visible in certain parts of the accessible tunnels. The main metals produced at Temperino mine were Cu, Pb, Zn and Ag. The mining activity is currently closed and a tourist route has been set up in the first level of the mine.

The muographic study involved the observation of a rock layer of about 50 m located between the first level of the Temperino mine and the Earth's surface. The aim of the measurements was to observe any low-density anomalies that could be linked to the presence of cavities above a particular area of the tourist route. Such cavities may be related to the presence of Radon gas measured in greater concentration in this area (within safety limits). Furthermore, the entire area above the gallery was subject to extensive mining activity during the Etruscan period, making probable the presence of ancient shafts or small-closed unknown cavities above the gallery, which were not taken into account during the more modern excavations as the extraction activity was concentrated at the lowest levels.

Two muographic measurements were taken at two different points along the tourist route in order to observe the area of interest from two different points of view. The results highlighted the presence of angular regions with low average density visible from both measurements. The densities observed in these areas have values lower than the typical rocks, and therefore, can be identified as cavities. Currently, the cavities have been located only angularly in two-dimensions. Studies for the three-dimensional localization are underway.

Knowledge of some cavities above the tourist route, in addition to explaining the presence of a higher concentration of Radon gas, is also important both from the safety of the tourist route and from the archaeological point of view. The three-dimensional reconstruction of any cavities can be inserted into a model for the evaluation of the stress–strain on the rocks, and in this way, it is possible to evaluate the risk factors for the stability of the tourist gallery.

Author Contributions: Conceptualization, D.B. (Diletta Borselli), T.B., L.B., V.C., R.D. C.F., S.G. (Sandro Gonzi) and A.P.; methodology, D.B. (Diletta Borselli), T.B., L.B., R.C.,V.C, R.D. C.F., S.G. (Sandro Gonzi) and A.P.; software, D.B. (Diletta Borselli), L.B. and S.G. (Sandro Gonzi); validation, D.B. (Diletta Borselli), T.B., L.B. D.B. (Debora Brocchini), V.C., R.F., A.D., G.G., S.G. (Sandro Gonzi), S.G. (Silvia Guideri), L.L, N.C., M.N. and S.V.; formal analysis, D.B. (Diletta Borselli), L.B., S.G. (Sandro Gonzi); investigation, D.B. (Diletta Borselli), T.B., L.B., D.B. (Debora Brocchini), A.D., G.G., S.G. (Sandro Gonzi), S.G. (Silvia Guideri), L.L., R.C., M.N. and S.V.; resources, L.B., T.B., D.B. (Debora Brocchini), R.C., V.C., R.D., G.G., N.C., L.L., M.N.; data curation, D.B. (Diletta Borselli), T.B. and L.B.; writing—original draft preparation, D.B. (Diletta Borselli); writing—review and editing, D.B. (Diletta Borselli), T.B., L.B., D.B. (Debora Brocchini), V.C., R.D., A.D., C.F, G.G., S.G. (Sandro Gonzi), S.G. (Silvia Guideri), L.L., M.N., A.P. and S.V.; visualization, D.B. (Diletta Borselli), T.B., L.B.; supervision, L.B., V.C. R.D. and N.C.; project administration, L.B., D.B. (Debora Brocchini), V.C., R.D., S.G. (Silvia Guideri); funding acquisition, D.B. (Diletta Borselli), T.B., L.B., D.B. (Debora Brocchini), V.C., R.D. and S.G. (Silvia Guideri). All authors have read and agreed to the published version of the manuscript.

Funding: This research is part of the MIMA-SITES ("Application of the Muon Imaging Technique in Archaeological and Mining Sites of Touristic and Historical Interest for the Evaluation of Cultural and Safety Aspects") project cofounded by the Tuscany Region (POR FSE 2014-2020) and Parchi Val di Cornia S.p.A., for the development of muon radiography in the cultural and safety field at the site of historical and tourist interest of the Temperino mine.

Informed Consent Statement: Informed consent was obtained from all subjects involved in the study.

Data Availability Statement: The raw data supporting the conclusions of this article will be made available, if needed, only for the purposes of peer review, because they are part of an ongoing study

Conflicts of Interest: The authors declare no conflicts of interest.

Abbreviations

The following abbreviations are used in this manuscript:

INFN	National Institute for Nuclear Physics
MIMA	Muon Imaging for Mining and Archaeology

References

1. Bonechi, L.; D'Alessandro, R.; Giammanco, A. Atmospheric muons as an imaging tool. *Rev. Phys.* **2020**, *5*, 100038. https://doi.org/10.1016/j.revip.2020.100038.
2. Tanaka, H.; Bozza, C.; Bross, A.; Cantoni, E.; Catalano, O.; Cerretto, G.; Giammanco, A.; Gluyas, J.; Gnesi, I.; Holma, M.; et al. Muography. *Nat. Rev. Methods Prim.* **2023**, *3*, 88. https://doi.org/10.1038/s43586-023-00270-7.
3. Alvarez, L. Search for Hidden Chambers in the Pyramids. *Science* **1970**, *167*, 832. https://doi.org/10.1126/science.167.3919.832.
4. Procureur, S.; Morishima, K.; Kuno, M.; Manabe, Y.; Kitagawa, N.; Nishio, A.; Gomez, H.; Attié, D.; Sakakibara, A.; Hikata, K.; et al. Precise characterization of a corridor-shaped structure in Khufu's Pyramid by observation of cosmic-ray muons. *Nat. Commun.* **2023**, *14*, 1144. https://doi.org/10.1038/s41467-023-36351-0.
5. Ambrosino, F.; Anastasio, A.; Basta, D.; Bonechi, L.; Brianzi, M.; Bross, A.; Callier, S.; Caputo, A.; Ciaranfi, R.; Cimmino, L.; et al. The MU-RAY project: detector technology and first data from Mt Vesuvius. *J. Instrum.* **2014**, *9*, C02029. https://doi.org/10.1088/1748-0221/9/02/C02029.
6. Oláh, L.; Hamar, G.; Ohminato, T.; Tanaka, H.K.; Varga, D. Branched Conduit Structure Beneath the Active Craters of Sakurajima Volcano Inferred From Muography. *JGR Solid Earth* **2024**, *129*, e2023JB028514. https://doi.org/10.1029/2023JB028514.
7. Holma, M.; Zhang, Z.; Kuusiniemi, P.; Loo, K.; Enqvist, T. Future Prospects of Muography for Geological Research and Geotechnical and Mining Engineering. *Geophys. Monogr. Ser.* **2022**, *15*, 199–219. https://doi.org/10.1002/9781119722748.ch15.
8. Beni, T.; Borselli, D.; Bonechi, L.; Lombardi, L.; Gonzi, S.; Melelli, L.; Turchetti, M.A.; Fanò, L.; D'Alessandro, R.; Gigli, G.; et al. Laser scanner and UAV digital photogrammetry as support tools for cosmic-ray muon radiography applications: an archaeological case study from Italy. *Sci. Rep.* **2023**, *13*, 19983. https://doi.org/10.1038/s41598-023-46661-4.
9. Borselli, D.; Beni, T.; Bonechi, L.; Bongi, M.; Ciaranfi, R.; Ciulli, V.; D'Alessandro, R.; Fanò, L.; Frosin, C.; Gonzi, S.; et al. Muography as a support technique for non-invasive research and three-dimensional localization of tombs in archaeological sites: A case study from Palazzone Necropolis (Perugia—Italy). *J. Instrum.* **2024**, *19*, C02076. https://doi.org/10.1088/1748-0221/19/02/C02076.
10. Liu, G.; Luo, X.; Tian, H.; Yao, K.; Niu, F.; Jin, L.; Gao, J.; Rong, J.; Fu, Z.; Kang, Y.; et al. High-precision muography in archaeogeophysics: A case study on Xi'an defensive walls. *J. Appl. Phys.* **2023**, *133*, 014901. https://doi.org/10.1063/5.0123337.
11. Grieder, P.K. *Cosmic Rays at Earth*; Elsevier: Amsterdam, The Netherlands, 2001.
12. Navas, S.; Particle Data Group. Review of Particle Physics. *Phys. Rev. D* **2024**, *110*, 030001. https://doi.org/10.1103/PhysRevD.110.030001.
13. Beni, T.; Borselli, D.; Bonechi, L.; Bongi, M.; Brocchini, D.; Ciaranfi, R.; Cimmino, L.; Ciulli, V.; D'Alessandro, R.; Dini, A.; et al. Transmission-Based Muography for Ore Bodies Prospecting: A Case Study from a Skarn Complex in Italy. *Nat. Resour. Res.* **2023**, *32*, 1529. https://doi.org/10.1007/s11053-023-10201-8.
14. Borselli, D.; Beni, T.; Bonechi, L.; Bongi, M.; Brocchini, D.; Casagli, N.; Ciaranfi, R.; Cimmino, L.; Ciulli, V.; et al. Three-dimensional muon imaging of cavities inside the Temperino mine (Italy). *Sci. Rep.* **2022**, *12*, 22329. https://doi.org/10.1038/s41598-022-26393-7.
15. Tioukov, V.; Alexandrov, A.; Bozza, C.; Consiglio, L.; D'Ambrosio, N.; De Lellis, G.; De Sio, C.; Giudicepietro, F.; Macedonio, G.; Miyamoto, S.; et al. First muography of Stromboli volcano. *Sci. Rep.* **2019**, *9*, 6695. https://doi.org/10.1038/s41598-019-43131-8.
16. Tioukov, V.; Morishima, K.; Leggieri, C.; Capriuoli, F.; Kitagawa, N.; Kuno, M.; Manabe, Y.; Nishio, A.; Alexandrov, A.; Gentile, V.; et al. Hidden chamber discovery in the underground Hellenistic necropolis of Neapolis by muography. *Sci. Rep.* **2023**, *13*, 5438. https://doi.org/10.1038/s41598-023-32626-0.
17. Frosin, C.; Ambrosino, F.; Andreetto, P.; Bonechi, L.; Bonomi, G.; Borselli, D.; Bottai, S.; Buhles, T.; Calliari, I.; Checchia, P.; et al. Exploring the potential of muon radiography for blast furnace assessments: advancements in non-invasive imaging and structural analysis. *J. Instrum.* **2024**, *19*, C02041. https://doi.org/10.1088/1748-0221/19/02/C02041.
18. Bonechi, L.; Ambrosino, F.; Andreetto, P.; Bonomi, G.; Borselli, D.; Bottai, S.; Buhles, T.; Calliari, I.; Checchia, P.; Chiarotti, U.; et al. BLEMAB European project: muon imaging technique applied to blast furnaces. *J. Instrum.* **2022**, *17*, C04031. https://doi.org/10.1088/1748-0221/17/04/C04031.
19. Borselli, D.; Ambrosino, F.; Andreetto, P.; Bonechi, L.; Bonomi, G.; Bottai, S.; Buhles, T.; Calliari, I.; Checchia, P.; Chiarotti, U.; et al. The BLEMAB European project: Muon radiography as an imaging tool in the industrial field. *Il Nuovo Cimento* **2022**, *45C*, 201. https://doi.org/10.1393/ncc/i2022-22201-x.

20. D'Alessandro, R.; Ambrosino, F.; Bonechi, L.; Cimmino, L.; Ireland, D.G.; Kaiser, R.; Mahon, D.; Mori, N.; Noli, P.; Saracino, G.; et al. Muography applied to nuclear waste storage sites. *Ann. Geophys.* **2017**, *60*, S0106. https://doi.org/10.4401/ag-7381.
21. Simpson, A.; Clarkson, A.; Gardner, S.; Al Jebali, R.; Kaiser, R.; Mahon, D.; Roe, J.; Ryan, M.; Shearer, C.; Yang, G. Muon tomography for the analysis of in-container vitrified products. *Appl. Radiat. Isot.* **2020**, *157*, 109033. https://doi.org/10.1016/j.apradiso.2019.109033.
22. Borgognoni, S.; Busino, M.; Guideri, S.; Fornaro, R.; Mattias, P. P.; Preite, M.; Savoca, D.; Zucconi, M. *Linee Guida per la Tutela, Gestione e Valorizzazione di Siti e Parchi Geominerari. Proposte e prospettive per la crescita e sostenibilità del settore*; ISPRA Manuali e linee guida 46/2008: Rome, Italy, 2008, ISBN 978-88-448-0359-9. Available online: https://www.isprambiente.gov.it/it/pubblicazioni/manuali-e-linee-guida/linee-guida-per-la-gestione-e-valorizzazione-di (accessed on 4 December 2024).
23. Dini, A.; Guideri, S.; Orlandi, P. *Miniere e Minerali del Campigliese. Il mondo sotterraneo del Parco di San Silvestro*; Gruppo Mineralogico Lombardo, Rivista Mineralogica Italiana (RMI), I Parchi della Val Cornia, Consiglio Nazionale delle Ricerche, Gruppo Mineralogico Lombardo: Milano, Italy, 2013; p. 98.
24. Carli, E. *Etruscan Mines. La Complessa Storia di un'Industria Mineraria*; Felici Editore: Pisa, Italy, 2010; ISBN: 9788860194091.
25. Kak, A.C.; Slaney, M. and Wang G. Principles of computerized tomographic imaging. *Med. Phys.* **2002**, *29*, 107. https://doi.org/10.1118/1.1455742.
26. Bonechi, L.; D'Alessandro, R.; Mori, N.; Viliani, L. A projective reconstruction method of underground or hidden structures using atmospheric muon absorption data. *J. Instrum.* **2015**, *10*, P02003. https://doi.org/10.1088/1748-0221/10/02/P02003.
27. Baccani, G.; Bonechi, L.; Borselli, D.; Ciaranfi, R.; Cimmino, L.; Ciulli, V.; D'Alessandro, R.; Fratticioli, C.; Melon, B.; Noli, P.; et al. The MIMA project. Design, construction and performances of a compact hodoscope for muon radiography applications in the context of archaeology and geophysical prospections. *J. Instrum.* **2018**, *13*, P11001. https://doi.org/10.1088/1748-0221/13/11/P11001.
28. Da Mommio, A.; Iaccarino, S.; Vezzoni, S.; Dini, A.; Rocchi, S.; Brocchini, D.; Guideri, S.; Sbrilli, L. Valorizzazione del geosito «Sezione Coquand», miniera del Temperino (Parco Archeominerario di San 1100 Silvestro, Campiglia Marittima). *Atti Della Soc. Toscana Sci. Nat. Mem. Ser. A* **2010**, *A*, 55–72. https://doi.org/10.2424/ASTSN.M.2010.07.
29. Bianchi, G. *Guida all'Archeologia Medievale Della Provincia di Livorno*; Nardini Editore: Florence, Italy, 2008.
30. Vezzoni, S.; Dini, A.; Rocchi, S. Reverse telescoping in a distal skarn system (Campiglia Marittima, Italy). *Ore Geol. Rev.* **2016**, *77*, 176–193. https://doi.org/10.1016/j.oregeorev.2016.03.001.